Journal of Controlled Release 381 (2025) 113619

Contents lists available at ScienceDirect

Journal of Controlled Release

journal homepage: www.elsevier.com/locate/jconrel

Wearable transdermal drug delivery system controlled by wirelessly powered acoustic waves

Jikai Zhang [a], Feixuan Yang [a], Haimeng Wu [a], Hui Ling Ong [a], Peter Arnold [a,e], Meng Zhang [b], Yunhong Jiang [b], Duygu Bahar [a], Zhishan Yuan [c], Xin Yang [d], Yong-Qing Fu [a,*]

[a] Faculty of Engineering and Environment, Northumbria University at Newcastle, Newcastle upon Tyne, NE1 8ST, UK
[b] Hub for Biotechnology in the Built Environment, Department of Applied Sciences, Faculty of Health and Life Sciences, Northumbria University at Newcastle, NE1 8ST, UK
[c] School of Electro-Mechanical Engineering, Guangdong University of Technology, Guangzhou 510006, China
[d] Department of Electrical and Electronic Engineering, School of Engineering, Cardiff University, Cardiff CF24 3AA, UK
[e] School of Biological Science, University of Leeds, LS2 9JT, UK

ARTICLE INFO

Keywords:
Surface acoustic wave
Drug delivery
Wireless powered
Wearable electronics
Transdermal drug delivery

ABSTRACT

Transdermal drug administration offers an alternative route for drug delivery through the skin, and surface acoustic wave (SAW) technology has recently emerged as a promising approach to enhance this process. However, conventional cable-connected SAW control units face several challenges, including inconvenience, poor wearability, limited miniaturization and integration, and restricted reusability. This study introduces a wireless-powered transport strategy for the transdermal delivery of large drug molecules using a thin-film-based SAW platform. This approach leverages interfacial acoustic stimulation, localized acoustic heating, and streaming/micro-cavitation to enhance drug penetration. By eliminating the need for physical connections, the wireless power transfer system reduces potential heating effects and localized tissue damage. To evaluate its performance, synthetic skin-like agarose gel and pig skin tissue were used as models. Hyaluronate rhodamine (5000 Da) was successfully delivered transdermally into pig skin tissue, achieving approximately 77.89 % of the efficiency observed with a conventional cable-connected SAW platform. These findings highlight wireless SAW technology as a promising alternative for enhancing transdermal drug delivery, offering a safer, more effective, and user-friendly therapeutic solution for patients.

1. Introduction

Historically, oral delivery has been the most commonly used drug administration route, with its benefits including convenience, cost-effectiveness and simplicity for both patients and doctors [1,2]. However, it presents several limitations. For example, its "first-pass" effect [3] causes a portion of the doses to be metabolized by the liver before reaching the target tissues [4,5]. While many drug molecules are stable in the acid and alkaline environments of digestive and circulation systems for long enough to reach the circulation, others are rapidly eliminated after their first pass through the liver and kidneys. Some drugs are not assimilated through the digestive system or may be destroyed by digestion. In many cases, the drug's residence time and effectiveness can be improved through its delivery through the skin, and varied compliance could be improved using transdermal drug delivery (TDD). For small hydrophilic molecules, such as hormones and nicotine, the TDD has recently become a major non-invasive method for drug administration [6–9]. However, TDD with a skin diffusion patch is often limited to small molecular weights or sizes, or highly lipophilic drugs. For example, commonly only those hydrophobic drug molecules less than 500 Da can be effectively and passively diffused through the stratum corneum (SC), the outermost layer of the epidermis [10,11]. In contrast, larger molecules or water-soluble molecules are generally unable to pass through the oily SC layers if without using large or highly energised physical forces.

To overcome the key challenges of TDD for large drug molecules, various active technologies have been developed [12,13], but most of these techniques have their own limitations. For example, microneedle-meditated administration could cause skin infections and localized erythema or edema [13]. Electrically driven techniques such as

* Corresponding author.
E-mail address: Richard.fu@northumbria.ac.uk (Y.-Q. Fu).

https://doi.org/10.1016/j.jconrel.2025.113619
Received 24 October 2024; Received in revised form 6 March 2025; Accepted 7 March 2025
Available online 9 March 2025

electrophoresis, phonophoresis or low-frequency ultrasonic methods could generate strong fields and cavitation effects on the skin surface, leading to potential damage including heat, skin burns, irritation, and tissue scarring on the applied areas [12,14]. Recently thin film-based surface acoustic wave (SAW) technology was developed in our group as an alternative for enhancing transdermal drug delivery [15]. These surface-propagating waves generate strong localized micro-mechanical agitation/streaming and acoustothermal effects at the skin surface, increasing the permeability of drug molecules into the stratum corneum layer and facilitating penetration of larger drug molecules up to millions of Daltons [15].

Although promising, SAW-enhanced TDDs face several key challenges, including design and miniaturization of complex control units, design and provision of medically acceptable wearable/flexible laminates, integration of wireless powered electronic control units, and design for reusability of expensive amplification and other electronics. For SAW technologies, high frequency (hundreds of MHz and above), wireless RF signal transmission has been widely applied in RF communication and sensing fields [16–18], whereas wireless SAW power transmission for achieving acoustofluidics or drug delivery has seldom been reported. Introducing such wireless SAW control circuits and power units should make SAW devices more flexible and miniaturized, but most importantly, provide patients with greatly improved comfort and mobility, and potentially reduce local damage and variable heat generation. Such issues commonly occur in the physically connected electronic circuits and electrodes through soldering and silver paint bonding processes. As previously reported, heating up to 45 degrees alters the permeability of skin, affecting the rheology of oils and proteins within the keratinized epidermis [19,20]. Wireless powering function can be effectively used to control heat generation within the defined parameters to maximize the SAW agitation effects independent of heat for the TDD. However, there are key technical challenges for wireless power transfer, such as enhancing efficiency, consistency, and reliability in device performance while minimizing power consumption and thermal effects.

In this study, we explore wireless-powered and SAW-controlled methods for drug transmission and achieve reliable and wireless functionalities within wearable prototypes. Hyaluronate rhodamine (HR) was selected as an example of the targeted drugs with high molecular weight hydrophilic molecules to demonstrate the effectiveness of a wireless-powered, flexible, and comfortable SAW patch for achieving efficient TDD. The design principle and mechanisms of the proposed wireless controlled system are illustrated in Fig. 1a, where a SAW patch is applied to the body and wirelessly controlled by a separate control and power box. The SAW patch is placed on the skin, and the control box which integrates the power supply is connected to the surface of the SAW patch via a replaceable adhesive gel layer. This setup allows it to transmit power and regulate its operation, enabling remote control of the system's functions without the need for wired connections. The structure of the drug patch is illustrated in Fig. 1b, in which several layers are integrated into the flexible platform, including a wireless power transfer (WPT) coil, a SAW device, and a layer of drug-hydrogel mixture attached to the skin surface. The WPT coil is positioned on the top layer to enable wirelessly receiving RF powers, while the SAW device beneath is used for activating the drug delivery. The hydrogel based adhesive layer at the bottom secures the entire structure to the target surface, allowing the patch to maintain its flexibility while performing its designated functions. The WPT control system is illustrated in Fig. 1c, where the primary side is consisted of a signal generator, amplifier, and a transmitter coil (Tx coil) paired with a capacitor (C_P). The receiver coil (Rx coil) and capacitor (C_S) receive the power in the resonant state to drive the SAW device as a load. To demonstrate the functionality and prove the concept, drug transdermal transmission experiments were conducted on agarose gels (as the synthetic skin-like material) and pig skins. We believe such a wireless-powered transdermal drug delivery patch could provide patients with a safer, more effective, lower-power required, and user-friendly solution.

2. Experimental

2.1. Materials and chemical preparation

To imitate skin, agarose gel was selected as a transparent and homogenous medium for demonstrating the performance of SAW-based drug delivery as its viscoelastic properties could be easily adjusted to mimic the elastic properties of human skin. In this study, 10 % agarose gel was selected as it was previously identified as being suitable for this application [21]. To prepare 10 % agarose gel, 10 g of agarose powders (Melford, UK, with its gel strength of 1200 g/cm^2) was mixed with 90 mL of de-ionized (DI) water. The solution was then heated in a 700 W

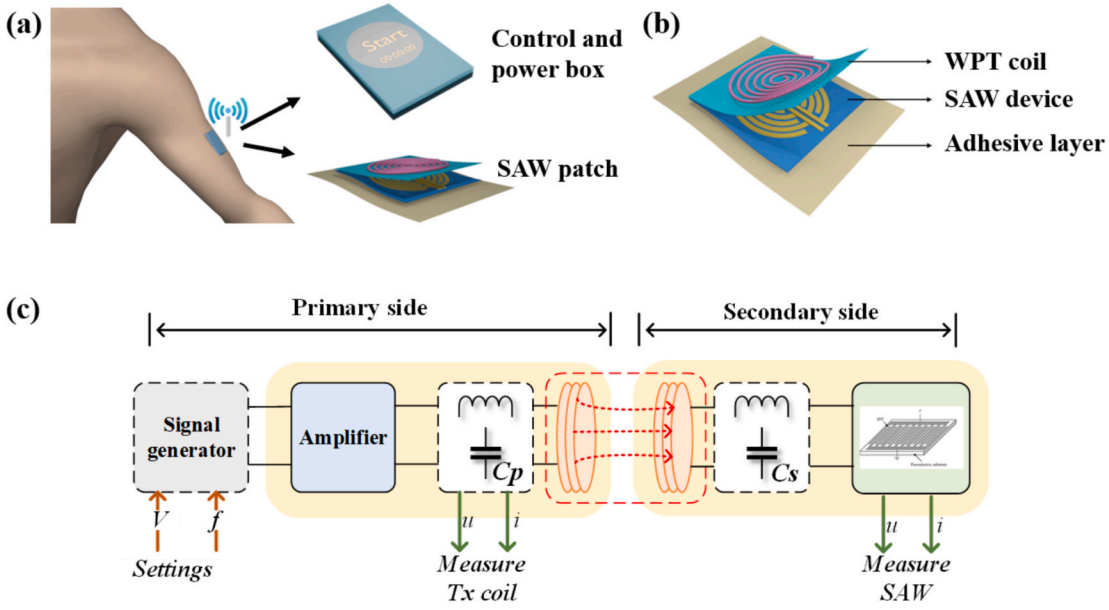

Fig. 1. Schematic illustrations of (a) design principles and operation mechanisms of SAW TDD systems; (b) The multilayer designs of the devices. (c) Wireless power transfer and control system.

microwave oven for one and half minute under a continuously stirring. The obtained mixture was poured into petri dishes for the agarose gel to be solidified.

For the drug delivery tests, hyaluronate rhodamine with a molecular weight of 5 kDa (hereafter abbreviated as HR, from Haworks, USA) was used. For each set, a batch of solutions (with a volume of 500 μL and a concentration of 0.1 mg/mL) were prepared by adding 0.05 mg of HR powder into 0.5 mL of DI water. Rh-Ha dyes with 0.01 mg/mL concentration were produced by mixing the above solution with 4.5 mL of ultrasound gel (UGEL250, Anagel, UK).

2.2. SAW device fabrication and characterization

ZnO thin film with a thickness of ~3.5 μm was deposited onto aluminum sheets (with a thickness of 200 μm) utilizing a direct current (DC) magnetron sputter (NS3750, Nordiko) and the details were previously reported in Ref. [15]. A zinc target with a purity of 99.99 % was used. During the film deposition, the substrate was positioned at ~20 cm away from the target, and mixed gases of argon and oxygen with an Ar/O_2 flow ratio of 10/20 were used. The DC plasma power was set at 350 W, and the chamber pressure was controlled to maintain at ~3.75 mTorr. X-ray diffraction (XRD) analysis using Siemens D5000 with Cu-Kα radiation, 40 kV, 30 mA showed that a sharp peak of ZnO (0002) with another peak from Al substrate within a two theta range from 30 to 60 degree, indicating c-axis texture and good crystallinity of the deposited ZnO film.

The interdigital transducers (IDTs) were patterned on the surface of ZnO thin film coated Al sheet using a conventional photolithography and lift-off process. A bilayer of Cr/Au was deposited to form the IDTs, with their thicknesses of 20 nm/100 nm, using a thermal evaporator (Edwards AUTO306). The IDTs were designed with a wavelength of 200 μm, comprising 30 pairs of electrodes. The reflection spectra (S11) of the SAW devices were measured using a network analyzer (Keysight, Field Fox N9913A). The resonant frequency (f_o) of the SAW devices was measured to be ~13.51 MHz using a network analyzer (N9913A, Keysight). At such frequency, the device can generate a mixture of Rayleigh and Lamb waves [14], which are used for transdermal drug delivery.

2.3. Wireless coils and matching circuit

A pair of wireless power transfer coils (1,461,798,021, Nucurrent, USA) were used with a diameter of 35.02 mm, a thickness of 0.68 mm and an inductance of 4 μH. They were chosen to match the performance of SAW devices, and the following formula was used to calculate the capacitance matching values used in the experimental designs [22].

$$j\left(\omega L_p - \frac{1}{\omega C_p}\right) = j\left(\omega L_s - \frac{1}{\omega C_s}\right) = 0 \tag{1}$$

where $\omega = 2\pi f$ is the angular frequency of the WPT system; f is the resonant frequency of the system; L_p and C_p are the inductance and capacitance values on the primary side of the WPT system, whereas L_s and C_s represent the inductance and capacitance values on the secondary side of the WPT system. The values of L and C can be adjusted using the following equation [22]:

$$f = \frac{1}{2\pi\sqrt{LC}} \tag{2}$$

When the coil matches the SAW device frequency used (13.50 MHz), the coupling capacitance was calculated to be ~37 pF. A capacitor with such the capacitance value was connected in series with the coil to meet the target frequency of ~13.50 MHz.

The receiver coil was soldered onto an SMA PCB connector to supply RF power. To determine the optimal coupling distance between the receiver and transmitter coil connected to the SAW device, the coil coupling distance was changed between 0.5 cm and 3 cm. The two coils were placed facing each other, and the distance between the transmitter and receiver coil was varied as illustrated in Fig. 2a. The primary side (transmitter coil side) of the WPT system was connected to one port of the network analyzer (ZNL3, Rohde and Schwarz, Germany), while the secondary side (receiver coil side) was connected to another port, as shown in Fig. 2b. The impedance and reflection amplitude (dB) values were measured at different distances between the coils and the best performance outputs were obtained. The transmission efficiency η of the WPT system was calculated from the S21 data (dB) measured using the network analyzer with the equation of $\eta = 10^{-\frac{dB}{20}}$. Fig. 2c shows the measured results of coupling coefficients and efficiency values as a function of distance between two coils. Notably, the efficiency reaches its maximum at approximately 1.5 cm. Fig. 2d shows the simulation results of the coupling coefficient as a function of the distance between the coils, which match well with the experimental results.

2.4. Drug delivery tests

The facilities used for the drug delivery tests included a power supply (RS Pro, PS-3005P), a signal generator (Aim-TTi, TGP3151 Pulse Generator), an RF amplifier (Mini-circuits, ZHL-5 W), and a DC power meter (9103, Racal Dana). The signal generator was used to produce RF signals with a frequency of 13.51 MHz and a variable peak-peak voltages or output powers, which were then input into the RF amplifier. The power output of the RF amplifier was connected to an RF power meter to reveal the nominated power supplied to the SAW devices, and the reflection power was not measured in this study. The applied voltages were from 578.0 mV to 849.0 mV, which were corresponding to the RF powers from 2.3 to 5.0 W. The SAW agitation durations were varied between 5 mins to 20 mins.

The agarose gel was cut into a square shape (~1.5 × 2 cm^2) with an average thickness of ~0.4 mm. The Rh-Ha gel paste of 0.1 mL was uniformly applied onto the agarose gel surface. The backside of the SAW device (i.e., the Al substrate side) was gently pressed onto the gel surface, fixed with metal pins to the pads of the SAW device. During the test, a thermocouple (2000 T, Digitron) was placed between the SAW device and gel surface to monitor the changes of surface temperature. After the test, the surface of gel sample was thoroughly cleaned using a fiber-free soft cloth to remove the remaining Rh-Ha dyes and then washed with running phosphate-buffered saline (PBS, Sigma-Aldrich) solution for 60 s for removal of any remaining Ra-Ha dyes. The gel was sectioned along the cross-section direction, and the slice thickness was controlled as ~0.1 mm.

Freshly market-available pig skin was cut into a uniform size (1.5 × 2 cm^2) using the same procedures as those for the agarose gel. The samples were fixed using the optimal cutting temperature (OCT, Scigen) compound and then sliced into a sample with a thickness of 30 μm using a low-temperature cryostat (−30 °C, 20 μm thickness, Model OTF/A5, with a bright field). Measurements of RH's fluorescence signals for both the agarose gel and pig skin samples were performed using a fluorescence microscope (DM5000B, Leica) with a laser wavelength of 488 nm under 50 and 100 times of magnifications. As the SC layer of pig skins contains corneocytes which has its natural fluorescence signal [23], this should be considered before the microscopical analysis of drug delivery depths of the tested pig skin samples. For this purpose, a square of untreated and fresh pig skin was also sectioned using the cryostat with the sample's sectioning parameters. Based on this result, the background intensity of the fluorescent microscope has been adjusted so that the background and natural fluorescence signals from the pig skin have been minimized. Further details can be found our previous publication [15].

The impedance of the pigskin surface was measured using an inductance, capacitance and resistance (LCR) meter (LCX100, Rohde & Schwarz, Germany). The LCR meter's electrodes were placed in direct contact with the pig skin surface and the resistance (R) readings were measured. Once the surface resistance was obtained, the resistivity (ρ)

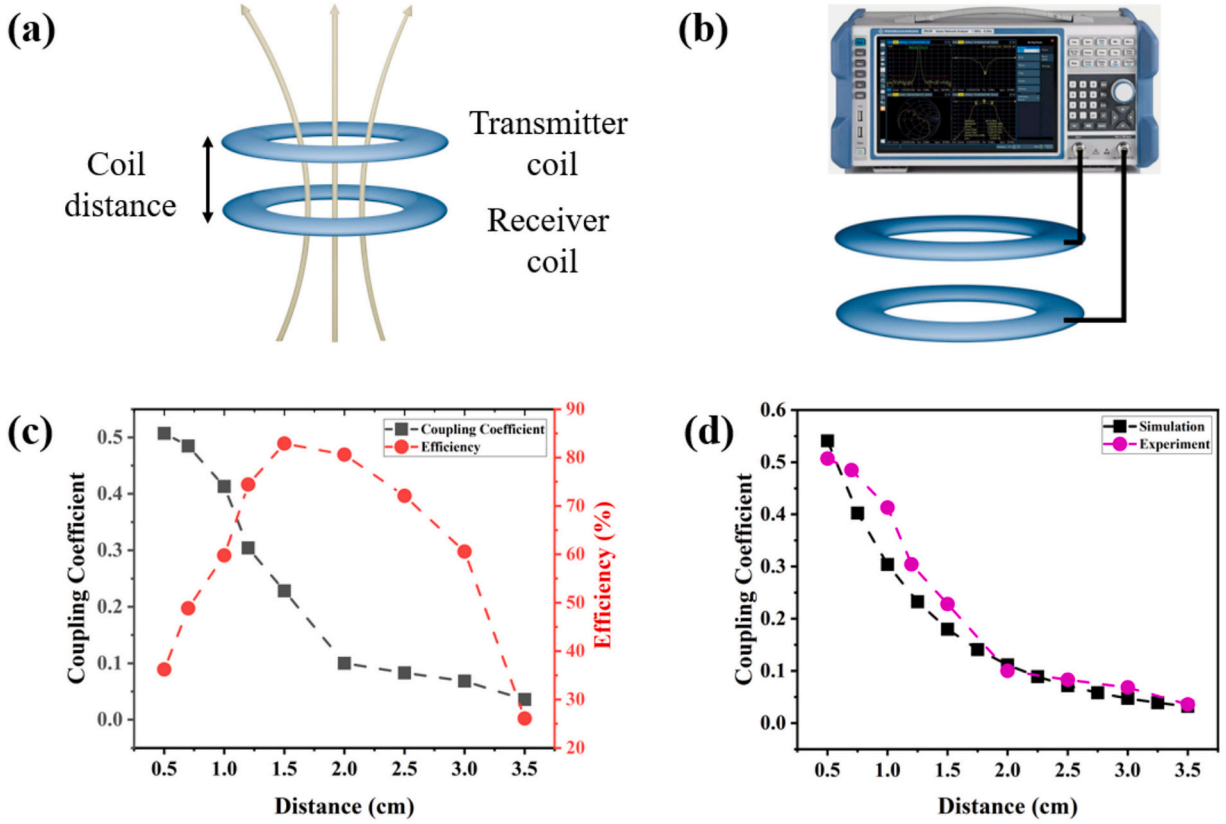

Fig. 2. WPT system: (a) Transmitter and receiver coil, (b) Network analyzer connection, (c) The coupling coefficient and efficiency with respect to the distance between the coils. (d) Simulation and experimental results of the coupling coefficient as a function of the distance between the coils.

was calculated using the following formula:

$$\rho = \mathbf{R} \times \frac{\mathrm{A}}{\mathrm{l}} \tag{3}$$

where ρ is the resistivity (in kΩ·cm); R is the measured resistance (in Ω), A is the cross-sectional area of the electrodes (in cm^2), and l is the distance between electrodes (in cm).

3. Results and discussions

3.1. Transmission efficiency and power calibration of wireless SAW devices

The coupling coefficients and efficiency values were obtained (see Fig. 2c) as a function of the distance between two coils. The coupling coefficient decreases significantly as the separation distance between the coils is increased. Similarly, the efficiency becomes increased as the distance is increased up to 1.5 cm, but then decreased as the coil distance is further increased from 1.5 cm to 3.5 cm. In this study, the power transfer efficiency reaches its maximum value when the coils are positioned at about 1.5 cm apart.

Simulation was performed to obtain the coupling coefficients as a function of the distance between the coils using the Ansys simulation software. In this simulation, a 3D model of the actual coils was constructed to mimic the experimental setup. The coil distance was systematically varied from 0.5 cm to 3.5 cm to investigate its influences on the coupling coefficients. Details of the simulations can be found in the Section I of the Supporting Information. The obtained simulation results are shown in Fig. 2d, and the coupling coefficient was found to decrease with increasing coil distance, aligning well with the experimental results (Fig. 2c). The distance of 1.5 cm was used in the following tests as the estimated optimum distance for achieving the maximum power transfer and minimized energy losses.

According to the frequency splitting theoretical framework, the operating region of a WPT system can be separated into undercoupled, critically coupled, and overcoupled states, based on the relationship between the actual coupling coefficient and the critical coupling coefficient [24–26]. At the distances shorter than 1.5 cm, the system is operated in the overcoupled region, where the strong coupling between the coils leads to a pronounced frequency splitting phenomenon. This is reflected in the experimental data, which shows an increase in power transfer efficiency as the distance approaches 1.5 cm, indicating a transition toward a critical coupling point. As the distance between the coils is increased from 1.5 cm to 3.5 cm, the coupling strength become gradually weakened, shifting the system toward the undercoupled region. Beyond this point of 1.5 mm, the efficiency declines significantly, consistent with the characteristics of the undercoupled state, where the achievable energy transmission efficiency is inherently limited [25].

To illustrate wave patterns and agitation effects induced by the SAW devices, finite element analysis (FEA) of the ZnO/Al SAW device was performed using COMSOL Multiphysics (6.2). The simulation parameters, including IDT configuration, material properties, and boundary conditions, are detailed in Section V of the Supporting Information. Fig. S5 shows the obtained acoustic pressure fields, which are characterized by alternating regions of positive and negative pressures of the propagating waves. The maximum pressure amplitude reaches approximately $\pm 2.5 \times 10^5$ Pa, with the pressure gradient concentrated at the IDT region. The energy is primarily coupled at the upper surface of the simulation model, gradually attenuated deeper into the skin. These simulation results demonstrate the efficiency of SAW excitation for producing localized high-energy zones, which are critical for enhancing transdermal drug delivery applications by facilitating enhanced permeability through the skin layers.

3.2. Thermal effect of SAW devices with wireless functions

The thermal effect generated by SAW agitation is well-documented [27]. We have studied the differences in thermal effects for the cases using the conventionally wired powering method and those using the wireless powering methods, and the obtained results are summarized in Fig. 3a and b. When applied with the same SAW power of 4.0 W for these cases, the surface temperatures, which were measured on the device using the conventionally used wired connection method, are generally ~16.6 °C higher than those using the wireless connected cases. The key reason for such temperature differences is the heating effect induced by the wired metal IDTs and also induced from the local power dissipation at the silver paint bonded region. These differences can be clearly seen from the thermal images as shown in Figs. 3c-3f. There is significant heating effects generated from those areas, where the IDTs were connected with cables through silver paints (see the marked Spot 1 in these figures), causing severe thermal effects. Whereas for the wireless connections between the SAW device and circuit, the thermal effects commonly generated at the IDT-connected region are insignificant, without posing as a critical issue. Another minor contribution for this difference is that the receiver coil receives slightly less energy during wireless transmission due to the reduced energy transfer efficiency during the wireless operation. When the transmitter coil was set at 4.00 W, the receiver coil could only receive a maximum power of 3.2 W. Fig. 3a and b show that when the wireless receiver coil power is 2.3 W (or 3.9 W with the wireless case), the temperature is about 23 % (or 62 %) lower than the corresponding wired power supply cases.

The above results clearly show that under the wireless power operation, the thermal effect on the surface of the SAW device can be effectively reduced. This is crucial for transdermal drug delivery as the excessive or uncontrolled large-scale heating has been the key concerns to damage the skin or alter properties of the drug molecules. Minimizing thermal effects can also enhance the overall reliability and extend the lifespan of the SAW device in applications.

3.3. TDD using agarose gel

Fig. 4(a) shows the measured transmission depths using the 5 kDa RH dyes into 10 % agarose gel as the skin model. The results were obtained at an RF power of 3.0 W for both the wired and wireless cases. The control group (i.e., without applying any SAWs) shows the lowest transdermal transmission depths for all the testing conditions. For

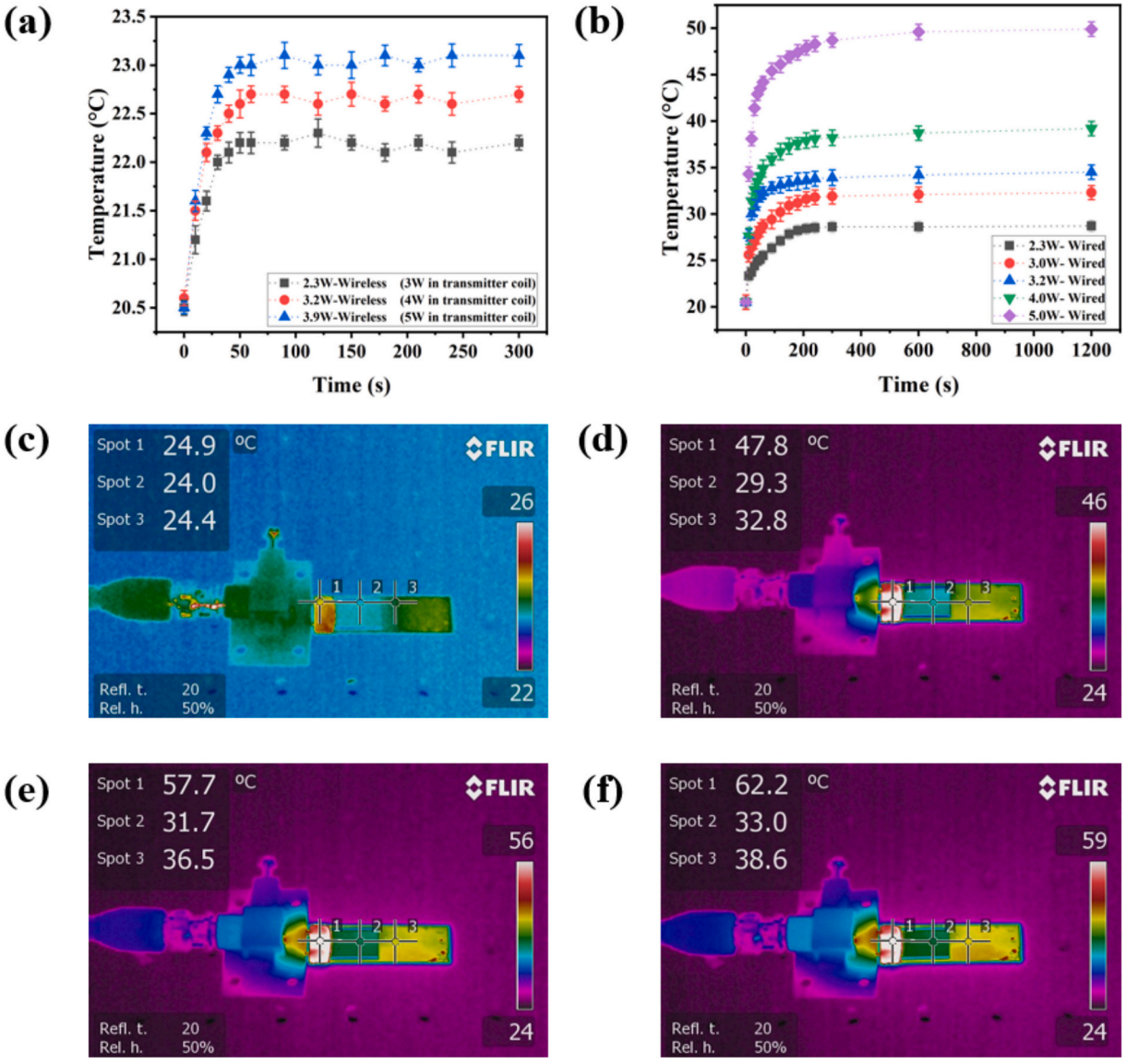

Fig. 3. Skin surface temperature in drug delivery experiments. (a) Wireless power (b) Wired power; Thermal image of the SAW device when the power is (c) 3.2 W in wireless conditions, (d) 2.3 W in wired conditions, (e) 3.2 W in wired conditions, (f) 4.00 W in wired conditions.

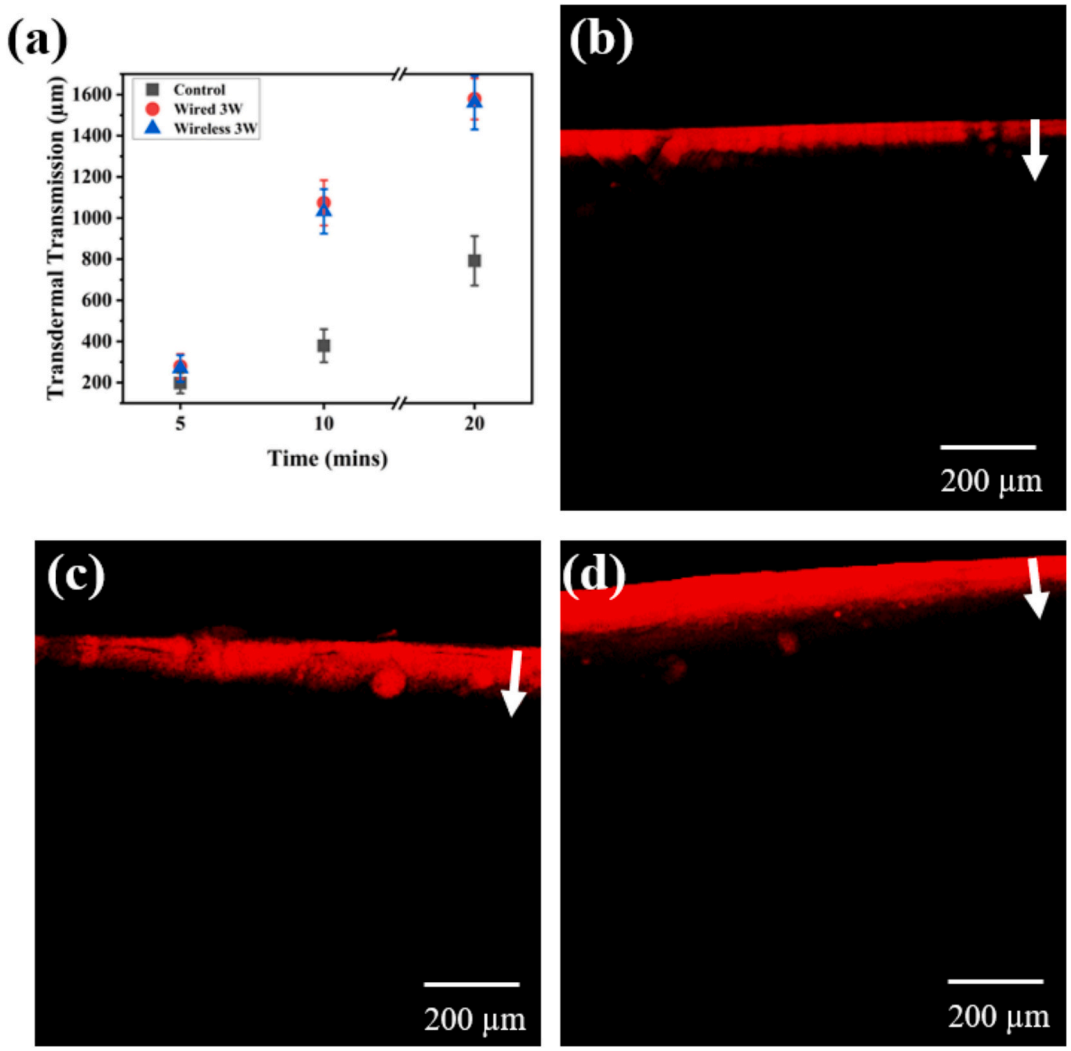

Fig. 4. (a) Transportation distances of 5 kDa Hyaluronate Rhodamine gel (0.1 mg/mL) into 10 % agarose gel at 3.0 W; Fluorescence images of (b) Control group in 5 mins; (c) Wireless case with a power of 3.0 W in 5 mins; (d) Wired case with a power of 3.0 W in 5 mins.

example, after 5 min, the transmission depth for the control group (0 W) was ~197 μm, but increased to ~378 μm after 10 min, and then reached ~792 μm at 20 min. This indicates that without using the SAW device, the diffusion is limited with a low rate of ~39.6 μm/min. In contrast, when using the conventional wired SAW device operated at an RF power of 3.0 W, there was a remarkable increase in transdermal transmission depth compared to that of the control group. After 5 min, the transmission depth was ~278 μm, nearly three times of that for the control group at the same operation duration. At this SAW power, the transmission depth reached ~1073 μm after 10 min and ~ 1578 μm after 20 min, corresponding to the delivery rates of ~107.3 μm/min and ~ 78.9 μm/min, respectively. The significantly increased delivery depths and fast rates demonstrate the effectiveness of the SAW enhancement in transdermal delivery of the RH dye.

Under the wireless operation, the SAW device with the applied RF power of 3.0 W also shows the enhanced transdermal transmission compared to the control group, although the obtained values were slightly lower than those from the wired device. For examples, after 5 min, the transmission depth was ~268 μm, which is substantially higher than the control group, although it is slightly lower than the wired device (~278 μm). However, we should address that the differences are not statistically significant. Figs. 4b to 4d show representative fluorescence images under the different testing conditions. The obtained fluorescence images can be found in the Section II of the Supporting Information. Our results showed that both the wired and wireless SAW devices significantly enhanced the transdermal transmission depths of the 5 kDa Rh-Ha dye in 10 % agarose gel compared to the control group. For example, in a 10-min test, the transmission depths were enhanced by approximately 173 % with the wired SAW device and 283 % with the wireless SAW device. Although the wired SAW device showed slightly larger transmission depths, the wireless device still demonstrated a substantial improvement if compared with the control group, validating its potential for effective transdermal drug delivery.

To verify if there is any micro-cavitation effect in this study, we used a high-speed camera (Hotshot 1280 CC, NAC image technology, Japan) to record the videos of cross-section microstructure changes of 1 % agarose gel layer under the applied SAW powers. An agarose gel sample of about $1 \times 1 \times 2$ cm^3 was placed on a 9.6 MHz SAW device, and was powered with 8 W. We have observed many micro-bubble formations and collapses within the gel, with examples shown in Figs. S4(a) - 2(d) in the supporting information. The bubbles were generated near the bottom of the gel once the acoustic waves were applied to the gel, and then they moved upward under the agitation of the acoustic waves. They appeared to burst around $t = 600$ ms as shown in Fig. S4(d). The corresponding video has been provided in the Supporting Information part IV.

3.4. TDD demonstrations using pig skin

The same SAW device was then used to conduct drug delivery experiments using the pig skin as the skin model. We applied the 5 KDa HR as the drug molecules for the TDD demonstration. Fig. 5a and b show the measured transmission depths of the drug molecules into the pig skin, using the wireless power supply and wired power supply, respectively. All the results were obtained by measuring the depths for ten times at different positions based on the fluorescence cross-section images and the average values from the repeated tests were obtained. The representative examples of fluorescence images are shown in Fig. 5c. The obtained fluorescence images are shown in the Supporting Information part III. Results showed that there is a strong correlation between the transmitter coil power and the transdermal transmission depth. The largest transmission depth was observed at a power of 3.9 W, at which the corresponding power in the transmitter coil was 5.0 W. After 20 min, the transmission distance with the highest power (3.9 W) was significantly larger (i.e., 56.81 μm) compared to those at a lower power level (i.e., 23.4 μm at 2.3 W) and the control group (9.59 μm).

When comparing the results for the wireless and wired systems at an RF power of 3.2 W, the wired cases clearly show larger transmission depths, although the difference is not substantial if compared with those of the wireless cases. For example, after 5 min, the depth was ~10.65 μm for the wireless case but it was ~22.80 μm for the wired cases. After 20-min, the depth was ~44.27 μm for the wireless one, and ~ 54.02 μm for the standard wired one. This difference is attributed to the reduced thermal effect and slightly smaller power transmission efficiency for the wireless case.

The possibility of skin surface damage using the wirelessly powered system was further investigated using both skin surface resistivity tests (Fig. 5d) and microscopic analysis of the cross-section skin morphology (Fig. 5e). The results from the resistivity tests (Fig. 5d) show that after applied with a SAW power of 3.2 W (for the wireless case) for 10 min, the resistivity of the skin surface did not show significant decreases, with an average resistivity value of 50 kΩ·cm. Based on the cross-section morphology analysis of the tissue structures, there were negligible differences in the overall morphologies before and after the SAW agitation experiments (see Fig. 5e).

To further investigate the potential effect under a large SAW power, we have subjected the skin surface with a high power of 10 W (with the wired case) for 10 min. There is an obvious damage to the skin surface. The epidermal wrinkles were clearly observed, mainly due to the moisture losses and temperature increases on the skin surface, with some areas even turned into dark yellow patches. As shown in Fig. 5e, some black dot-like protrusions were observed, which was mainly caused by the protein denaturation under the increased temperature and high RF powers. Concurrently, the surface resistivity reading showed a significant decrease to a value of ~20 kΩ·cm, indicating that applying a very high power could cause damage to the skin surface. In our study for drug delivery into skins, we did not use such a high power of 10 W.

All the above results clearly show that both wireless and wired power transfer system results show that increasing power levels lead to greater transdermal transmission distances, demonstrating the effectiveness of SAW in enhancing drug delivery. For all the cases, longer exposure times

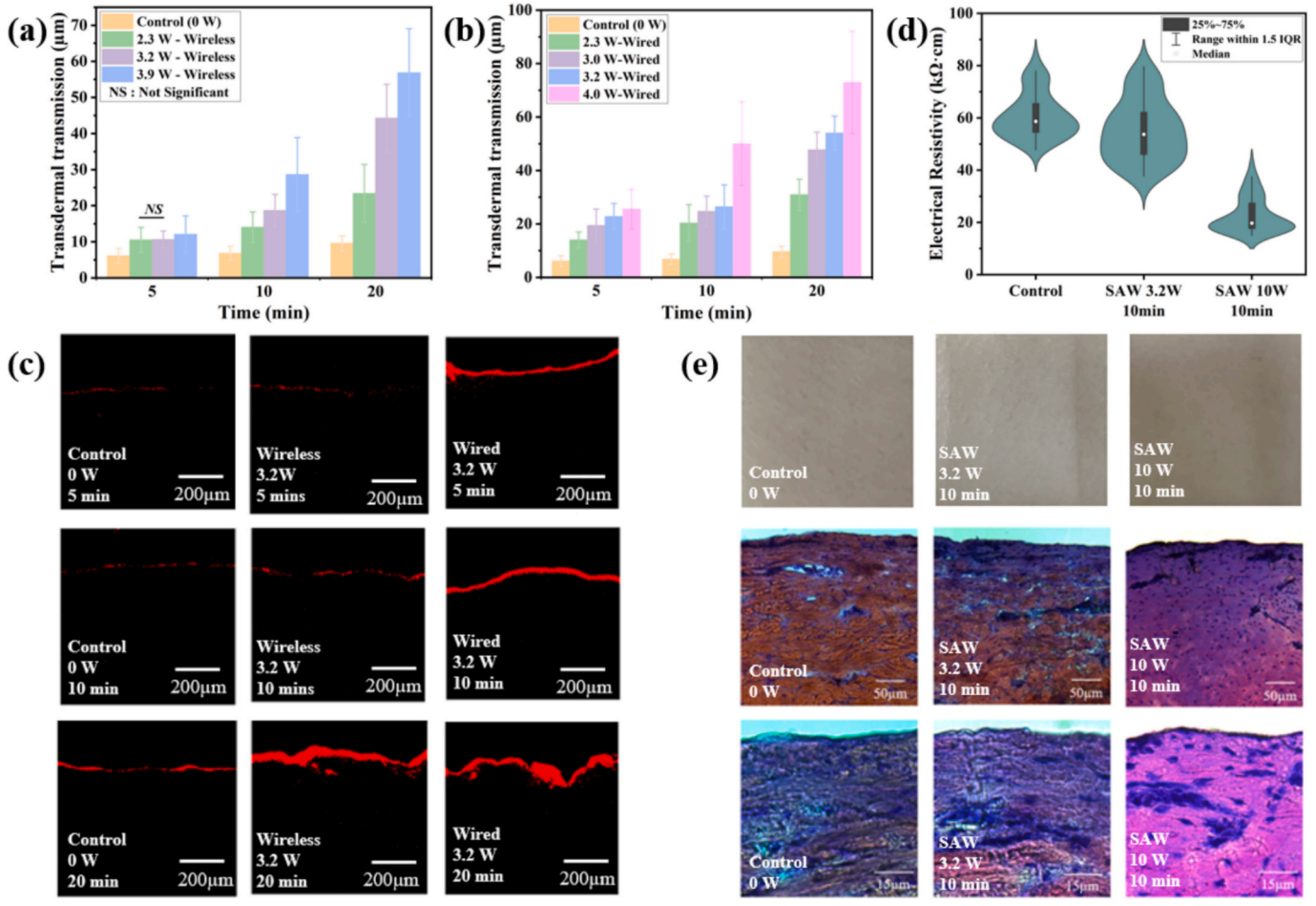

Fig. 5. Delivery depths of 5 kDa Hyaluronate Rhodamine molecules (0.1 mg/mL) into pig skin under the agitation of SAWs using (a) wireless power (b) wired power. By comparisons, there are statistically significant differences ($p < 0.05$), except for the one labelled NS; (c) Typical examples of fluorescence images of transportation distances. (d) Pig skin surface electrical resistivity test. (e) Surface morphology and tissue sections of pig skin before and after the experiment.

lead to increased transmission depths (see Fig. 4c). Despite the slightly lower transmission distances, the wireless SAW setup shows its great potential for transdermal drug delivery, offering notable advantages in terms of reduced heat generation and improved safety.

As it is well-known that the epidermis of human skin presents the main barrier to protect internal tissues from external penetrations [7,28]. The outermost oily SC layer of 15 to 20 μm thick is consisted of multiple layers of dead and keratinized cells [29]. Penetration through this barrier is possible if molecules are oily and small, but it is commonly expected that large hydrophilic water-soluble materials do not pass readily through the skin [30–33]. It is possible to break the epidermis layer for drug delivery with microneedles, electrothermal, or ultrasound methods. However, those methods tend to cause surface damage and have often shown adverse effects [28,34]. SAWs offer a novel approach by inducing nanoscale vibrations that temporarily disturb the SC layers, creating transient channels for drug diffusion [15], through mechanisms including localized suction generated by the mini earthquake-like vibrations on the skin surface, facilitating the transmission of drug molecules within minutes. We should address that the SAW induced heating effect could also alter the top structure of skin, making fats more liquid and altering viscosity [20,35]. While excessive heating could pose a risk of thermal damage, our findings suggest that controlled and localized heating induced by SAWs aids in deforming lipid structures in the SC. This enhances drug molecule penetration without causing significant damage, striking a balance between efficacy and safety.

In this study, we showed that the wireless controlled power transmission system offers several advantages. The wireless system significantly reduced heat generation compared to its wired counterpart, minimizing thermal damage. SAW devices have the great capability to deform lipidic structures in the SC, aided by localized heating and acoustic pressure, thus enhancing the efficient drug molecule penetration. This supports the design of portable, flexible, and wireless controlled TDD devices that are aligned with the portability requirements necessary for practical applications.

4. Conclusions

This study was mainly focused on wireless-powered SAW enhanced transdermal drug delivery. Through well-defined experimentation employing both agarose gel and real pig skin tissue, we have proven the potential of wireless powered SAWs in facilitating the transport of large drug molecules weighing 5 kDa through the epidermis layer. Our findings highlighted the significant roles of wireless power transmission in minimizing thermal effects and optimizing the efficiency of the drug delivery system. Lower operating temperatures contributed to greater patient comfort and safety, making the drug delivery process more tolerable for extended usages. Additionally, this study investigated the energy transmission efficiency of wireless devices, providing insights into the optimization of coil coupling distance for maximum power transfer. Overall, the research demonstrates the potential of wireless SAW technology as a promising alternative for enhancing transdermal drug delivery, offering a safer, more effective, and user-friendly solution for patients.

Declaration of generative AI and AI-assisted technologies in the writing process

Statement: During the preparation of this work, the author(s) used ChatGPT 4.0 to improve the readability and language of the manuscript. After using this tool, the authors reviewed and edited the content as needed and took full responsibility for the content of the published article.

CRediT authorship contribution statement

Jikai Zhang: Writing – review & editing, Writing – original draft, Visualization, Project administration, Methodology, Investigation, Formal analysis, Data curation, Conceptualization. **Feixuan Yang:** Writing – original draft, Software, Formal analysis. **Haimeng Wu:** Writing – review & editing, Resources. **Hui Ling Ong:** Writing – review & editing. **Peter Arnold:** Writing – review & editing. **Meng Zhang:** Writing – review & editing, Resources. **Yunhong Jiang:** Writing – review & editing. **Duygu Bahar:** Formal analysis. **Zhishan Yuan:** Writing – review & editing, Resources. **Xin Yang:** Resources. **Yong-Qing Fu:** Writing – review & editing, Supervision, Funding acquisition, Conceptualization.

Acknowledgement

This research was supported by the Northern Accelerator CCF Feasibility and Proof of Concept program. Key financial support was provided by Northumbria University through internal Proof-of-Concept funding. Additionally, we acknowledge the Innovation-to-Commercialization of University Research (ICURe) Program for their support in conducting market research. We also greatly appreciated for the help from students of Ayman Rizwan, Kieran Leniewski, and our business manager, Dr. Chelsea Brain, during the experimental work and project discussions.

Data availability

All data generated during this study are included in this published article and its supplementary information files.

References

[1] H. Park, A. Otte, K. Park, Evolution of drug delivery systems: From 1950 to 2020 and beyond, J. Control. Release 342 (2022) 53–65, https://doi.org/10.1016/j.jconrel.2021.12.030.
[2] P. Verma, A.S. Thakur, K. Deshmukh, A.K. Jha, S. Verma, Routes of drug administration, Int. J. Pharm. Stud. Res. 1 (2010) 54–59. https://romanpub.com/resources/ijpsr%20v11-2020-7.pdf (accessed August 3, 2024).
[3] E. Moroz, S. Matoori, J.-C. Leroux, Oral delivery of macromolecular drugs: where we are after almost 100 years of attempts, Adv. Drug Deliv. Rev. 101 (2016) 108–121, https://doi.org/10.1016/j.addr.2016.01.010.
[4] Frontiers | Advances in Oral Drug Delivery. https://www.frontiersin.org/journals/pharmacology/articles/10.3389/fphar.2021.618411/full, 2025 (accessed August 3, 2024).
[5] J. Deng, X. Zhu, Z. Chen, C.H. Fan, H.S. Kwan, C.H. Wong, K.Y. Shek, Z. Zuo, T. N. Lam, A review of food–drug interactions on oral drug absorption, Drugs 77 (2017) 1833–1855, https://doi.org/10.1007/s40265-017-0832-z.
[6] F. Sabbagh, B.S. Kim, Recent advances in polymeric transdermal drug delivery systems, J. Control. Release 341 (2022) 132–146, https://doi.org/10.1016/j.jconrel.2021.11.025.
[7] W.Y. Jeong, M. Kwon, H.E. Choi, K.S. Kim, Recent advances in transdermal drug delivery systems: a review, Biomater. Res. 25 (2021) 24, https://doi.org/10.1186/s40824-021-00226-6.
[8] D. Ramadon, M.T.C. McCrudden, A.J. Courtenay, R.F. Donnelly, Enhancement strategies for transdermal drug delivery systems: current trends and applications, Drug Deliv. Transl. Res. 12 (2022) 758–791, https://doi.org/10.1007/s13346-021-00909-6.
[9] J. He, Y. Zhang, X. Yu, C. Xu, Wearable patches for transdermal drug delivery, Acta Pharm. Sin. B 13 (2023) 2298–2309, https://doi.org/10.1016/j.apsb.2023.05.009.
[10] A.M. Vargason, A.C. Anselmo, S. Mitragotri, The evolution of commercial drug delivery technologies, Nat. Biomed. Eng. 5 (2021) 951–967, https://doi.org/10.1038/s41551-021-00698-w.
[11] S. Adepu, S. Ramakrishna, Controlled drug delivery systems: current status and future directions, Molecules 26 (2021) 5905, https://doi.org/10.3390/molecules26195905.
[12] H. Marwah, T. Garg, A.K. Goyal, G. Rath, Permeation enhancer strategies in transdermal drug delivery, Drug Deliv. 23 (2016) 564–578, https://doi.org/10.3109/10717544.2014.935532.
[13] J. Chen, H. Ren, P. Zhou, S. Zheng, B. Du, X. Liu, F. Xiao, Microneedle-mediated drug delivery for cutaneous diseases, Front. Bioeng. Biotechnol. 10 (2022), https://doi.org/10.3389/fbioe.2022.1032041.
[14] S. Ramesan, A.R. Rezk, L.Y. Yeo, High frequency acoustic permeabilisation of drugs through tissue for localised mucosal delivery, Lab Chip 18 (2018) 3272–3284, https://doi.org/10.1039/C8LC00355F.
[15] J. Zhang, D. Bahar, H.L. Ong, P. Arnold, M. Zhang, Y. Jiang, R. Tao, L. Haworth, X. Yang, C. Brain, M. Rahmati, H. Torun, Q. Wu, J. Luo, Y.-Q. Fu, Flexible surface acoustic wave technology for enhancing transdermal drug delivery, Drug Deliv. Transl. Res. (2024), https://doi.org/10.1007/s13346-024-01682-y.

[16] W. Liu, K.T. Chau, X. Tian, H. Wang, Z. Hua, Smart wireless power transfer—opportunities and challenges, Renew. Sust. Energ. Rev. 180 (2023) 113298. https://www.sciencedirect.com/science/article/pii/S1364032123001545 (accessed August 11, 2024).
[17] P. Lu, M. Wagih, G. Goussetis, N. Shinohara, C. Song, A comprehensive survey on transmitting antenna systems with synthesized beams for microwave wireless power transmission, IEEE J. Microw. 3 (4) (2023) 1081–1101 (accessed August 11, 2024), https://ieeexplore.ieee.org/abstract/document/10177162/.
[18] S. Olenik, H.S. Lee, F. Güder, The future of near-field communication-based wireless sensing, Nat. Rev. Mater. 6 (2021) 286–288, https://doi.org/10.1038/s41578-021-00299-8.
[19] J.-H. Park, J.-W. Lee, Y.-C. Kim, M.R. Prausnitz, The effect of heat on skin permeability, Int. J. Pharm. 359 (2008) 94–103, https://doi.org/10.1016/j.ijpharm.2008.03.032.
[20] J. Hao, P. Ghosh, S.K. Li, B. Newman, G.B. Kasting, S.G. Raney, Heat effects on drug delivery across human skin, Expert Opin. Drug Deliv. 13 (2016) 755–768, https://doi.org/10.1517/17425247.2016.1136286.
[21] Flexible surface acoustic wave technology for enhancing transdermal drug delivery, Drug Deliv. Transl. Res. 15 (2025) 1363–1375. https://link.springer.com/article/10.1007/s13346-024-01682-y (accessed August 11, 2024).
[22] J. Hu, J. Zhao, F. Gao, A real-time maximum efficiency tracking for wireless power transfer systems based on harmonic-informatization, IEEE Trans. Power Electron. 38 (2023) 1275–1287, https://doi.org/10.1109/TPEL.2022.3200096.
[23] D.C. Carrer, C. Vermehren, L.A. Bagatolli, Pig skin structure and transdermal delivery of liposomes: a two photon microscopy study, J. Control. Release 132 (2008) 12–20, https://doi.org/10.1016/j.jconrel.2008.08.006.
[24] A.P. Sample, D.T. Meyer, J.R. Smith, Analysis, experimental results, and range adaptation of magnetically coupled resonators for wireless power transfer, IEEE Trans. Ind. Electron. 58 (2010) 544–554. https://ieeexplore.ieee.org/abstract/document/5437250/ (accessed September 12, 2024).
[25] R. Huang, B. Zhang, D. Qiu, Y. Zhang, Frequency splitting phenomena of magnetic resonant coupling wireless power transfer, IEEE Trans. Magn. 50 (2014) 1–4. https://ieeexplore.ieee.org/abstract/document/6971783/ (accessed September 12, 2024).
[26] D.-W. Seo, J.-H. Lee, H.-S. Lee, Optimal coupling to achieve maximum output power in a WPT system, IEEE Trans. Power Electron. 31 (2016) 3994–3998, https://doi.org/10.1109/TPEL.2015.2504625.
[27] Y. Wang, Q. Zhang, R. Tao, D. Chen, J. Xie, H. Torun, L.E. Dodd, J. Luo, C. Fu, J. Vernon, P. Canyelles-Pericas, R. Binns, Y. Fu, A rapid and controllable acoustothermal microheater using thin film surface acoustic waves, Sensors Actuators A Phys. 318 (2021) 112508, https://doi.org/10.1016/j.sna.2020.112508.
[28] V. Phatale, K.K. Vaiphei, S. Jha, D. Patil, M. Agrawal, A. Alexander, Overcoming skin barriers through advanced transdermal drug delivery approaches, J. Control. Release 351 (2022) 361–380, https://doi.org/10.1016/j.jconrel.2022.09.025.
[29] S. Olsztyńska-Janus, A. Pietruszka, Z. Kiełbowicz, M. Czarnecki, ATR-IR study of skin components: lipids, proteins and water. Part I: Temperature effect, Spectrochim. Acta A Mol. Biomol. Spectrosc. 188 (2018) 37–49. https://www.sciencedirect.com/science/article/pii/S1386142517305504 (accessed September 9, 2024).
[30] D. Bird, N.M. Ravindra, Transdermal drug delivery and patches—an overview, Med. Dev. Sens. 3 (2020) e10069, https://doi.org/10.1002/mds3.10069.
[31] E. Touitou, Drug delivery across the skin, Expert. Opin. Biol. Ther. 2 (2002) 723–733, https://doi.org/10.1517/14712598.2.7.723.
[32] A. Alexander, S. Dwivedi, T.K. Ajazuddin, S. Giri, S. Saraf, D.K. Tripathi Saraf, Approaches for breaking the barriers of drug permeation through transdermal drug delivery, J. Control. Release 164 (2012) 26–40, https://doi.org/10.1016/j.jconrel.2012.09.017.
[33] C. Pegoraro, S. MacNeil, G. Battaglia, Transdermal drug delivery: from micro to nano, Nanoscale 4 (2012) 1881–1894, https://doi.org/10.1039/C2NR11606E.
[34] M.R. Prausnitz, R. Langer, Transdermal drug delivery, Nat. Biotechnol. 26 (2008) 1261–1268. https://www.nature.com/articles/nbt.1504 (accessed September 9, 2024).
[35] S. Szunerits, R. Boukherroub, Heat: a highly efficient skin enhancer for transdermal drug delivery, Front. Bioeng. Biotechnol. 6 (2018) 15. https://www.frontiersin.org/articles/10.3389/fbioe.2018.00015/full (accessed September 9, 2024).